OFFICE OF NAVAL RESEARCH

Contract: N00014-85-K-0222

Work Unit: 4327-555

Scientific Officer: Dr. Richard S. Miller

Technical Report No. 23

INTERNAL FAILURES IN MODEL ELASTOMERIC COMPOSITES

by

A.N. Gent and Y.-C. Hwang

College of Polymer Science Polymer Engineering
The University of Akron
Akron, Ohio 44325

November, 1989

SECURITY CLASSIFICATION OF THIS PAGE (When Data Entered)

REPORT DOCUMENTATION PAGE		READ INSTRUCTIONS BEFORE COMPLETING FORM
1. REPORT NUMBER Technical Report No. 23	2. GOVT ACCESSION NO.	3. RECIPIENT'S CATALOG NUMBER
4. TITLE (and Subtitle) Internal Failures in Model Elastomeric Composites		5. TYPE OF REPORT & PERIOD COVERED Technical Report 6. PERFORMING ORG. REPORT NUMBER
7. AUTHOR(s) A.N. Gent and Y.-C. Hwang		8. CONTRACT OR GRANT NUMBER(s) N00014-85-K-0222
9. PERFORMING ORGANIZATION NAME AND ADDRESS Polymer Engineering Center The University of Akron Akron, Ohio 44325		10. PROGRAM ELEMENT, PROJECT, TASK AREA & WORK UNIT NUMBERS 4327-555
11. CONTROLLING OFFICE NAME AND ADDRESS Office of Naval Research Power Program Arlington, VA 22217-5000		12. REPORT DATE November 1989 13. NUMBER OF PAGES 35
14. MONITORING AGENCY NAME & ADDRESS(if different from Controlling Office)		15. SECURITY CLASS. (of this report) Unclassified 15a. DECLASSIFICATION/DOWNGRADING SCHEDULE

16. DISTRIBUTION STATEMENT (of this Report)

According to Attached distribution list.
Approved for public release; distribution unrestricted.

17. DISTRIBUTION STATEMENT (of the abstract entered in Block 20, if different from Report)

18. SUPPLEMENTARY NOTES

Submitted for publication in: Journal of Materials Science

19. KEY WORDS (Continue on reverse side if necessary and identify by block number)

Composites, Cracking, Elastomers, FEM, Fracture, Internal Failures, Rubber

20. ABSTRACT (Continue on reverse side if necessary and identify by block number)

Finite element methods have been used to calculate the rate of release of strain energy caused by growth of an internal crack in some model elastic composites under tension. A layer of a linearly-elastic material was considered, bonded between two flat or two spherical rigid surfaces. The reduction in strain energy caused by a small circular crack at the interface was found to be only about one-half of that due to a similar crack in the center

DD FORM 1 JAN 73 1473 EDITION OF 1 NOV 65 IS OBSOLETE
S/N 0102-LF-014-6601

SECURITY CLASSIFICATION OF THIS PAGE (When Data Entered)

of the layer, in accord with the conjecture of Andrews and King (11). Cracks in the center of a thin layer bonded between flat surfaces caused about the same release of energy as a crack in the center of a thick specimen under the same tensile stress. On the other hand, a crack in a thin layer bonded between two spherical surfaces caused a much larger rate of energy release, depending on the radius of the layer relative to its minimum thickness. Growth of an initial crack would thus occur at a small applied stress. For thin layers between both flat and spherical surfaces, the rate of release of energy decreased as the crack grew, indicating that the crack would stabilize at a finite size. These conclusions are in accord with some observations of cracks in thin elastic layers (8,9).

Accession For	
NTIS GRA&I	☒
DTIC TAB	☐
Unannounced	☐
Justification	
By	
Distribution/	
Availability Codes	
Dist	Avail and/or Special
A-1	

1. Introduction

Cracks grow when there is enough mechanical energy available in the system to drive them forward. This is the Griffith fracture criterion: that energy released by crack growth must be sufficient to meet the energy requirements of a growing crack, termed the fracture energy of the material and denoted here G_c (1,2). We have calculated the rate of release of strain energy for a circular crack, of radius c, growing in a layer of an elastic material bonded between two rigid spheres, Figure 1, or two rigid flat surfaces, Figure 2. The crack is placed either in the center of the elastic layer, Figures 1a and 2a, or at the center of the interface between one rigid material and the elastic layer, Figures 1b and 2b. The first corresponds to an internal crack in the elastomeric material and the second to a defect in adhesion. The corresponding measures of strength are G_c units of energy required to tear through unit area of material and G_a units of energy for debonding unit area of interface.

The elastic material is assumed to be linearly-elastic and virtually incompressible. Finite element methods are used to calculate the stiffness of the models for various sizes of the crack, and hence the strain energy W corresponding to a given applied force and deflection. In this way the reduction ΔW in strain energy brought about by the presence of the crack is evaluated for various crack radii.

A crack will grow if the rate of reduction in strain energy at constant deflection is sufficiently large, i.e., if

$$\partial(\Delta W)/\partial c \geq 2\pi c G_c \text{ (or } 2\pi c G_a). \qquad (1)$$

We have evaluated the quantity on the left-hand side of Equation 1 numerically, for a wide range of geometrical shapes. The results are presented here. They enable us to calculate the critical loads at which cracks of a given size will grow, when the fracture energy $\underline{G}_c$ or $\underline{G}_a$ is known. Some conclusions are also drawn on the final size of cracks formed between two rigid surfaces.

Cracks are initiated in two ways. They occur naturally, as defects within the material or at the bonded interface. Measurements of the strength of rubbery materials suggest that "natural" flaws or stress-raisers equivalent to sharp cracks, about 50 μm in size, are always present (3,4). Cracks are also formed within an elastomer by internal fracture under a dilatant stress (5). Any small void within an elastomeric solid will expand elastically without limit when a critical level of triaxial tension $\underline{-P}$ is applied, of about $\underline{5E/6}$, where $\underline{E}$ is the tensile (Young) modulus of elasticity (5,6). In practice, the void bursts open to form an internal crack when

$$-P \geq 5E/6. \qquad (2)$$

This critical condition is readily set up in elastomeric composites near rigid boundaries. For example, cracks appear abruptly near the poles of an isolated rigid spherical inclusion, in the direction of applied tension, when the local triaxial tension reaches the critical value (7,8). When two rigid spheres are located close together in the direction of an applied tension, then a crack appears in the elastomer layer midway between them

when the critical condition is reached there (8,9). Indeed, it seems that a crack always forms where, and when, the critical dilatant stress is set up.

We now turn to the question of the applied stress at which cracks will grow and the size that they will eventually attain. These questions are independent of the origin of the cracks themselves, but in considering them we also are led to consider the question of which criterion is met first, Equation 1, for growth of an initial defect, or Equation 2, for bursting open of an initial void.

2. Analytical procedures

A finite element arrangement with cylindrical symmetry was employed, using 400 elements. It is shown schematically for a center crack of radius c in Figures 3 and 4. In this case only one-half of the complete unit was modeled, but for a single interfacial crack at one surface it was necessary to model the complete unit. Calculations were carried out using the ADINA code (10), the material between the end-pieces being assumed to be linearly-elastic with a value of Poisson's ratio ν of either 0.4999 or 0.49, corresponding to extreme values for rubber compounds.

Values of applied force F were computed for unit deflection of the model and hence the elastic strain energy W was obtained, given by $F/2$. These values were smaller, of course, than the value W_o when no crack was present, and they decreased as the radius c of the crack was made larger, becoming zero when the radius of a central crack reached the radius a of the specimen or

when the interfacial crack became equal in size to the original bonded area.

Values of the reduction ΔW, relative to the value W_o in the absence of a crack, are plotted in Figures 5-8 as a function of the crack radius c, relative to the radius a of the specimen. Four representative cases are shown: thin and thick elastic layers bonded between spherical end-pieces (Figures 5 and 6), and thin and thick elastic layers bonded between flat end-pieces (Figures 7 and 8).

3. Results and discussion

(1) Small cracks in thin elastic layers

When the crack was extremely small in comparison with the radius a of the specimen, then the reduction ΔW in strain energy that it caused was too small to determine with any accuracy. As the value of c was increased, a linear relation was found to hold between $\log \Delta W$ and $\log c$, as can be seen in Figures 5-8, with a slope of 3 in this representation. Thus, when the crack size was small in comparison with the specimen radius,

$$\Delta W/W_o = (c/\ell)^3, \tag{3}$$

where ℓ is a characteristic length of the stress distribution in elastic layers. ℓ may be regarded as an inverse measure of the sensitivity of the stress distribution to the presence of a crack. Large values of ℓ correspond to small reductions in elastic strain energy for a crack of given size.

Values of $\underline{\ell}$ determined from relations like those shown in Figures 5-8 are given in Table 1 for various thicknesses $\underline{h}$ of the elastic layer. They were found to be virtually the same for the two values of Poisson's ratio used here, 0.49 and 0.4999. No distinction is made hereafter between the two results.

Values of $\underline{\ell}$ are plotted against the thickness $\underline{h}$, relative to the radius $\underline{a}$ of the cylindrical specimen, in Figures 9 and 10, using logarithmic scales for both axes. In this representation they follow linear relations initially, with a slope of unity, corresponding to a direct proportionality between $\underline{\ell}$ and $\underline{h}$:

$$\ell = \alpha h \,, \tag{4}$$

Values of the constant of proportionality $\underline{\alpha}$ are given in Table 2.

They were close to unity in all cases, indicating that the characteristic length $\underline{\ell}$ of the stress distribution in thin bonded layers is similar in magnitude to the thickness $\underline{h}$ of the layer itself. However, they were clearly smaller for cracks growing in the center of the elastic layer than for interfacial cracks of the same size. Thus, from Equation 3, more energy is released by a central crack than by an interfacial crack. From the computed values of $\underline{\ell}$, we deduce that about twice as much energy is released by a central crack, Table 1. This is consistent with the conclusion of Andrews and King (11), that the rate of release of strain energy near a rigid boundary is only one-half of that for a central crack because only one-half as much material is made stress-free as the crack grows.

(ii) Small cracks in thick elastic layers

When the layer thickness h was relatively large, of the same order as the radius a of the specimen or larger, then the characteristic length ℓ no longer followed a direct proportionality with h. Instead, it tended to increase more slowly, as shown in Figures 9 and 10. The logarithmic relations shown there at large values of h have slopes of 1/3, corresponding to

$$\ell = \beta h^{1/3}. \qquad (5)$$

The coefficients β were found to be in satisfactory agreement with theoretical values, derived below, of 0.92 for a center crack and 1.13 for an interfacial crack.

(iii) Theoretical result for a small crack in a thick layer

Sack's solution for the breaking stress σ_b of a long cylindrical specimen containing a small central crack of radius c takes the form (12),

$$\sigma_b^2 = \pi E G_c / 3c, \qquad (6)$$

where E is the tensile (Young) modulus of elasticity of the material. Substituting in terms of the strain energy W_o and strain energy density U, i.e., the strain energy per unit volume in regions remote from the crack, where

$$U = \sigma_b^2 / 2E$$

and

$$W_o = \pi a^2 h(\sigma_b^2/2E),$$

and employing the Griffith criterion for propagation of a circular crack of radius c, Equation 1, we obtain

$$\Delta W = 4c^3 U, \tag{7}$$

corresponding to

$$\Delta W/W_o = (4/\pi)c^3/a^2 h. \tag{8}$$

Thus, a small crack in the center of a long cylindrical block in tension causes a reduction in strain energy given by Equations 7 and 8. On comparing Equations 3 and 8, the characteristic length ℓ is given by

$$\ell = (\pi a^2/4)^{1/3} h^{1/3}. \tag{9}$$

Analogous relations for an interfacial crack take the form

$$\bar{\sigma}_b^2 = 2\pi E G_a/3c,$$

$$\Delta W = 2c^3 U,$$

and

$$\Delta W/W_o = (2/\pi)c^3/a^2 h$$

in place of Equations 6, 7 and 8.

Thus, the observed form of the dependence of ℓ upon h for thick layers is accounted for, and a theoretical value obtained from

Equations 5 and 9 for the coefficient β [$= (\pi a^2/4)^{1/3}$ for a central crack and $(\pi a^2/2)^{1/3}$ for an interfacial crack]. A quantitative comparison of these values of β with the calculated results is made in Figures 9 and 10. Values of β for cracks in thick elastic layers are seen to be in satisfactory agreement with the theoretical values when h/a is greater than unity, for specimens with either spherical or flat end-pieces, containing either central or interfacial cracks. Thus, both the form and magnitude of the computed rate of release of strain energy by a small crack in a thick elastic layer are in reasonable agreement with analytical solutions. This agreement lends support to the other results, when complete analytical solutions are not available.

(iv) Large cracks

The computed relations for reduction ΔW in strain energy, Figures 5-8, show interesting differences as the crack radius c is made larger. They depart from a proportionality to c^3, but deviate in different ways, depending upon the layer thickness h. For relatively thin layers, Figures 5 and 7, they become much less sensitive to crack size, approaching a constant value, i.e., becoming largely independent of c as c approaches its maximum possible value, the radius a of the cylindrical specimen. For thick elastic layers, on the other hand, Figures 6 and 8, the rate of release of strain energy by a growing crack stays constant or increases when the crack radius becomes large. These differences suggest that a crack growing in a thin layer will slow down and stop, because the rate of release of strain energy becomes less,

whereas a similar crack growing in a thick layer will accelerate, in view of the increasing rate at which energy becomes available to it.

(v) Predicted loads at which a small initial crack in a thin elastic layer will grow

Equations 3 and 4 lead directly to a condition for growth of an initial crack of radius $\underline{c}$ in terms of the strain energy $\underline{W}_o$

$$W_o \geq (2\pi/3)\alpha^3 h^3 G_c/c \qquad (10)$$

using the Griffith fracture criterion, Equation 1. Now, approximate relations are available for the stiffness, and hence strain energy $\underline{W}_o$, of thin bonded elastic layers. For example, for a layer bonded between two flat plates, with a radius $\underline{a}$ much larger than the thickness $\underline{h}$, we have (13,14)

$$F = \pi a^4 E\delta/2h^3 \qquad (11)$$

and for a thin layer bonded between two rigid spheres (15,16),

$$F = \pi a^2 E\delta/2h. \qquad (12)$$

On substituting for $\underline{W}_o$ in Equation 10, critical values for the mean applied stress $\bar{\sigma}$ ($\underline{= F/\pi a^2}$), denoted $\bar{\sigma}_c$, are obtained as

$$\bar{\sigma}^2_c \geq 2\alpha^3 E G_c/3c \qquad (13)$$

and

$$\bar{\sigma}_c^2 \geq 2\alpha^3 (h/a)^2 EG_c/3c, \qquad (14)$$

respectively.

Recalling that the coefficient α is approximately equal to unity, Equation 13 indicates that a small crack within a thin bonded layer will grow at a mean applied tensile stress of about the same magnitude as that for a large sample containing a crack of the same size, Equation 6. There is little effect of proximity of bonded planes on the tendency of a crack to propagate. But Equation 14 shows that a crack in an elastic layer bonded between two closely-spaced rigid spheres is much more likely to grow. In this case, the critical stress is reduced by the ratio h/a of sphere spacing to radius. For example, if the spacing h is one-tenth of the radius a, then the fracture stress will be only one-tenth of the regular tensile breaking stress.

However, for closely-spaced spheres the rate of release of strain energy falls off markedly as the crack grows, Figure 5. Thus, although a crack will start to grow at a low stress, it will not continue to propagate until the sample is severed. Instead, it will stabilize at a finite size. This is precisely what is observed (9).

(vi) Crack growth or void expansion?

Equation 13 applies to a pre-existing crack in a thin layer bonded between flat surfaces. Unless the crack is unusually large, it predicts a much greater critical stress than for unbounded expansion of a pre-existing void by a dilatant stress, Equation 2. For example, if E is given a value of 2 MPa,

representative of soft elastomeric solids, and G_c is given a value of 1 kJ/m^2, typical of reasonably strong rubbery solids, then the fracture stress is calculated from Equation 13 to be about 7.5 MPa, when the initial crack radius is assumed to be 25μm and putting $\alpha = 1$. On the other hand, the mean applied stress at which a critical dilatant stress of 5E/12 is reached in the center is only about 0.9 MPa. Thus, void expansion is likely to be the first mechanism of internal fracture encountered in stretching thin bonded layers, unless they contained exceptionally large initial cracks.

For a thin layer bonded between spherical surfaces, the critical stress for crack growth is much smaller, by the factor h/a, Equation 14. Previous analyses have shown that the maximum dilatant stress $-P_m$ set up in the center of a thin layer is increased in inverse proportion, relative to the mean applied stress (15,16),

$$-P_m/\bar{\sigma} = a/h \ ,$$

so that the critical stress $\bar{\sigma}_c$ for void expansion will be reduced by the same factor. Thus, the relative tendency for growth of an initial crack compared to expansion of an existing void is not changed. Both processes are made easier, and by the same factor, in a thin layer bonded between spherical surfaces. Again. therefore, void expansion is likely to be the first failure encountered.

In the above discussion, failure by debonding at the interface has been ignored. As shown previously, stresses for interfacial

failure will be higher than for growth of a central crack if the fracture energies are similar. Thus, only if the interface is much weaker than the material itself (or if the interface contains unusually large debonds) will debonding occur before void formation.

4. Conclusions

(a). Griffith's fracture criterion for growth of a circular crack of radius c is given in Equation 1. For small cracks in thin bonded layers, the left-hand side of this relation, $\partial(\Delta W)/\partial c$, is given approximately by $3W_o c^2/h^3$, where h is the layer thickness, i.e., the minimum distance separating the rigid bonded surfaces. For small cracks in thick layers this term is given approximately by $3W_o c^2/a^2 h$, where a is the radius of the layer. Thus, the effective volume of the specimen, from which energy is released by crack growth, is given approximately by h^3 in the first case and by the volume of the entire layer ($\pi a^2 h$) in the second.

(b). In thin layers, the dependence of this term on c becomes much smaller as the crack grows. Thus a crack will reach a stable size eventually, without causing the specimen to break in two. In thick layers, on the other hand, once the condition for crack growth is met a crack will grow catastrophically.

(c). The reduction in strain energy caused by an interfacial crack is only one-half of that caused by a central crack of the same size. Thus, other things being equal, a central crack will grow preferentially

(d). Simple finite element analyses provide useful information about fracture in model systems, like those considered here, that

are somewhat too complicated to be amenable to solution in closed form and yet seem sufficiently general to be of wide application.

Acknowledgements

This work was supported by a grant from the Office of Naval Research (Contract N00014-85-K-0222; Project Officer Dr. R.S.Miller) and by grants-in-aid from Lord Corporation and Westvaco. The authors are also indebted to Professor R.A.Schapery of Texas A and M University for helpful comments on computations in these systems.

References

1. A.A.Griffith, Phil.Trans.Roy.Soc.(Lond.) A221, 163-198 (1920).
2. A.A.Griffith, Proc.1st Internatl.Congr.Appl.Mech., Delft, pp.55-63 (1924).
3. P.B.Lindley and A.G.Thomas, Proc.4th Internatl.Rubb.Conf., London, pp.428-442 (1962).
4. A.N.Gent, P.B.Lindley and A.G.Thomas, J.Appl.Polym.Sci. 8, 455-466 (1964).
5. A.N.Gent and P.B.Lindley, Proc.Roy.Soc.(Lond.) A249, 195-205 (1958).
6. A.E.Green and W.Zerna, "Theoretical Elasticity", Oxford Univ. Press, London, 1960, Section 3.10.
7. A.E.Oberth and R.S.Bruenner, Trans.Soc.Rheol. 9(2), 165-185 (1965).
8. A.N.Gent and B.Park, J.Mater.Sci. 19, 1947-1956 (1984).
9. K.Cho and A.N.Gent, J.Mater.Sci. 23, 141-144 (1988).
10. K.-J.Bathe, "ADINA: A finite Element Program for Automatic Dynamic Incremental Non-Linear Analysis", Report No.82448-1, M.I.T., Cambridge, MA., 1977.
11. E.H.Andrews and N.E.King, J.Mater.Sci. 11, 2004-2014 (1976).
12. R.A.Sack, Proc.Phys.Soc.(Lond.) 58, 729-736 (1946).
13. A.N.Gent and P.B.Lindley, Proc.Instn Mech.Engrs.(Lond.) 173, 111-122 (1958).
14. A.N.Gent and E.A.Meinecke, Polym.Eng.Sci. 10, 48-53 (1970).
15. A.N.Gent and B.Park, Rubb.Chem.Technol. 59, 77-83 (1986).
16. A.N.Gent and Y.-C.Hwang, Rubb.Chem.Technol. 61, 630-638 (1988).

Table 1: Values of $\underline{\ell}$ for various thicknesses $\underline{h}$ of an elastic layer bonded between two spherical or two flat surfaces. $\underline{\ell}_i$ and $\underline{\ell}_c$ denote values for interfacial and center cracks respectively.

Spherical end-pieces

$\underline{a/h}$	$\underline{\ell}_i$	$\underline{\ell}_i$	$\underline{\ell}_c$	$\underline{\ell}_c$
	$\underline{\nu}$ = 0.4999	0.49	0.4999	0.49
50	0.032	---	0.026	---
10	0.16	---	0.12	---
5	0.30	---	0.22	---
1	0.98	0.98	0.75	0.73
0.5	1.31	1.36	1.06	1.15
0.1	2.41	2.31	2.15	2.00

Flat end-pieces

$\underline{a/h}$	$\underline{\ell}_i$	$\underline{\ell}_i$	$\underline{\ell}_c$	$\underline{\ell}_c$
	$\underline{\nu}$ = 0.4999	0.49	0.4999	0.49
50	0.028	---	0.022	---
10	0.104	---	0.085	---
5	0.21	---	0.16	---
1	0.89	0.97	0.67	0.67
0.5	1.53	1.60	1.00	1.02
0.1	----	2.37	2.10	2.06

Table 2: Coefficient α of the relationship, $\ell = \alpha h$, for thin bonded layers. α_i and α_c denote values for interfacial and center cracks respectively.

	α_i	α_c
Spherical surfaces	1.58	1.26
Flat surfaces	1.07	0.87

Figure Legends

1. (a) A center crack and (b) an interfacial crack in an elastic layer bonded between rigid spherical end-pieces.

2. (a) A center crack and (b) an interfacial crack in an elastic layer bonded between rigid flat plates.

3. Sketch of finite element arrangements for an elastic layer containing a center crack, bonded between two rigid spheres.

4. Sketch of finite element arrangements for an elastic layer containing a center crack, bonded between two rigid plates.

5. Computed values of reduction ΔW in original elastic energy W_o due to the presence of a crack of radius c. Filled circles, interfacial crack; open circles, center crack. Spherical end-pieces, radius a and separation h; $h/a = 0.1$.

6. Computed values of reduction ΔW in original elastic energy W_o due to the presence of a crack of radius c. Filled circles, interfacial crack; open circles, center crack. Spherical end-pieces, radius a and separation h; $h/a = 2$.

7. Computed values of reduction ΔW in original elastic energy W_o due to the presence of a crack of radius c. Filled circles, interfacial crack; open circles, center crack. Flat end-pieces, radius a and separation h; $h/a = 0.1$.

8. Computed values of reduction ΔW in original elastic energy W_o due to the presence of a crack of radius c. Filled circles, interfacial crack; open circles, center crack. Flat end-pieces, radius a and separation h; $h/a = 2$.

9. Scaling parameter ℓ for small cracks in an elastic layer bonded between rigid spherical end-pieces, obtained from initial linear relations like those shown in Figures 5 and 6, plotted

against the relative thickness h/a of the elastic layer. Filled circles, interfacial cracks; open circles, center cracks.

10. Scaling parameter ℓ for small cracks in an elastic layer bonded between two rigid flat end-pieces, obtained from initial linear relations like those shown in Figures 7 and 8, plotted against the relative thickness h/a of the elastic layer. Filled circles, interfacial cracks; open circles, center cracks.

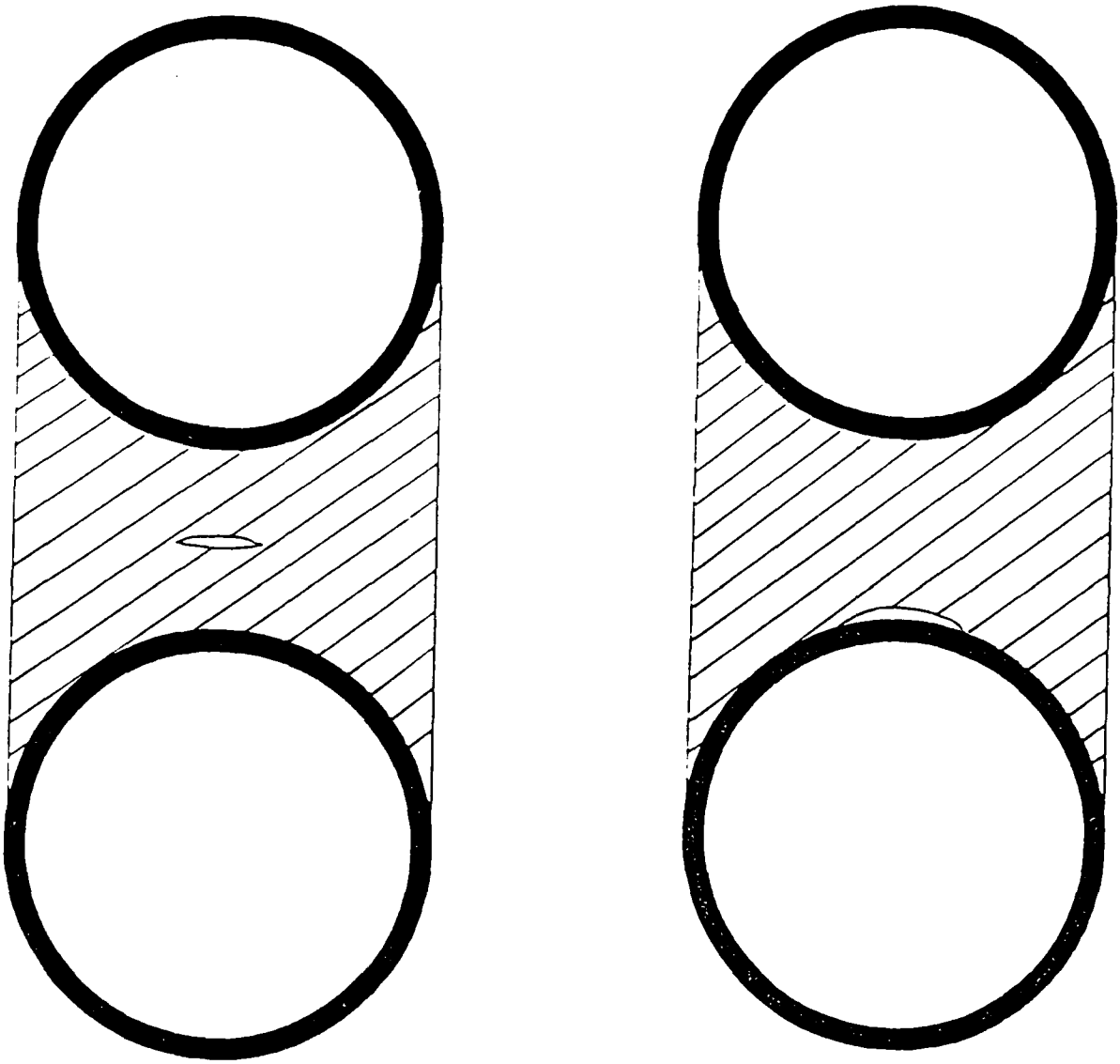

Figure 1

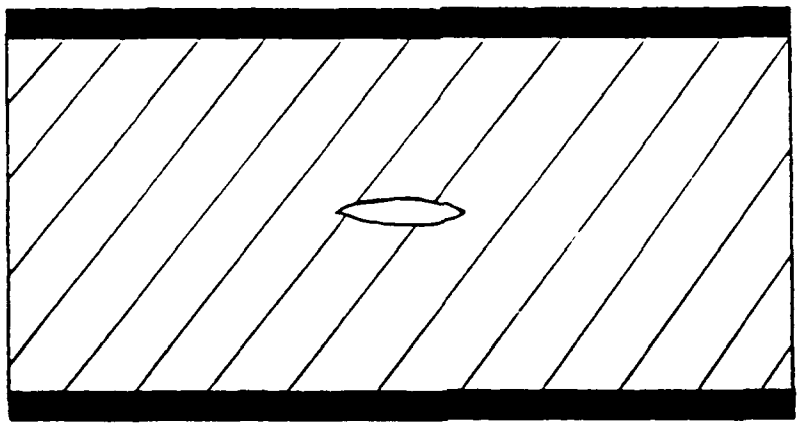

(a)

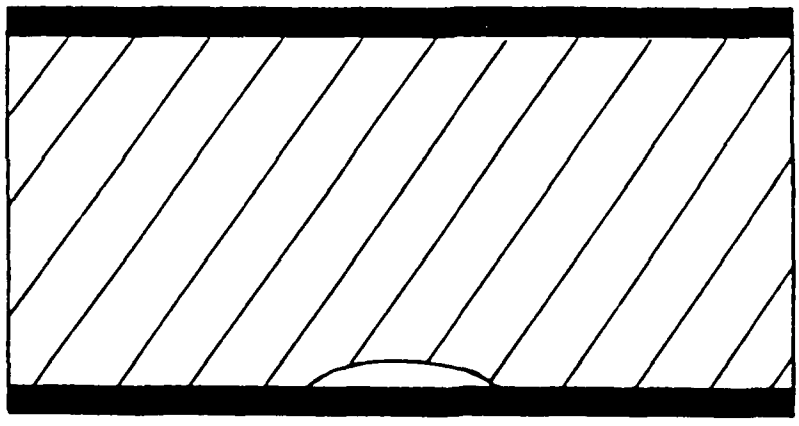

(b)

Figure 2

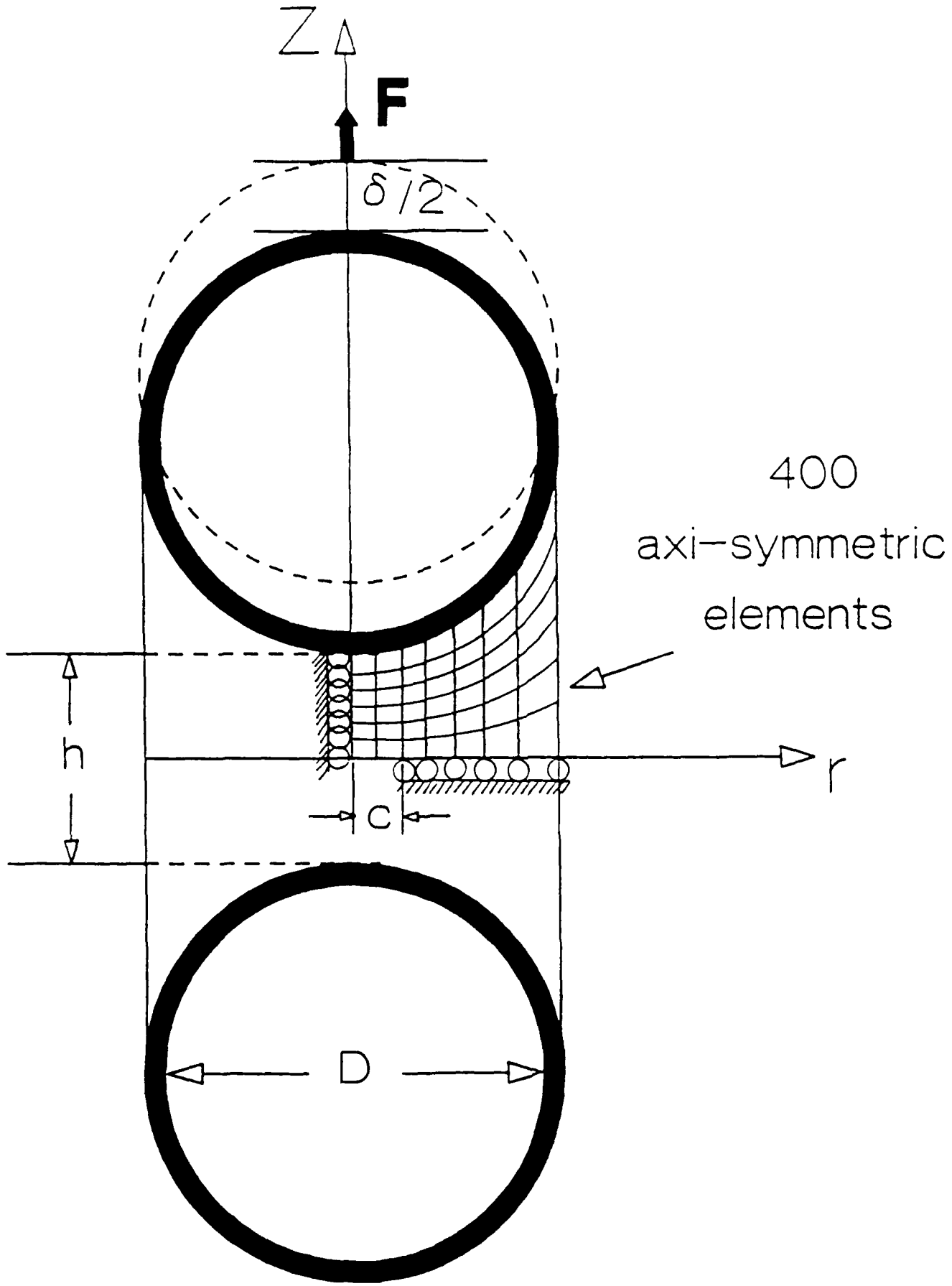

Figure 3

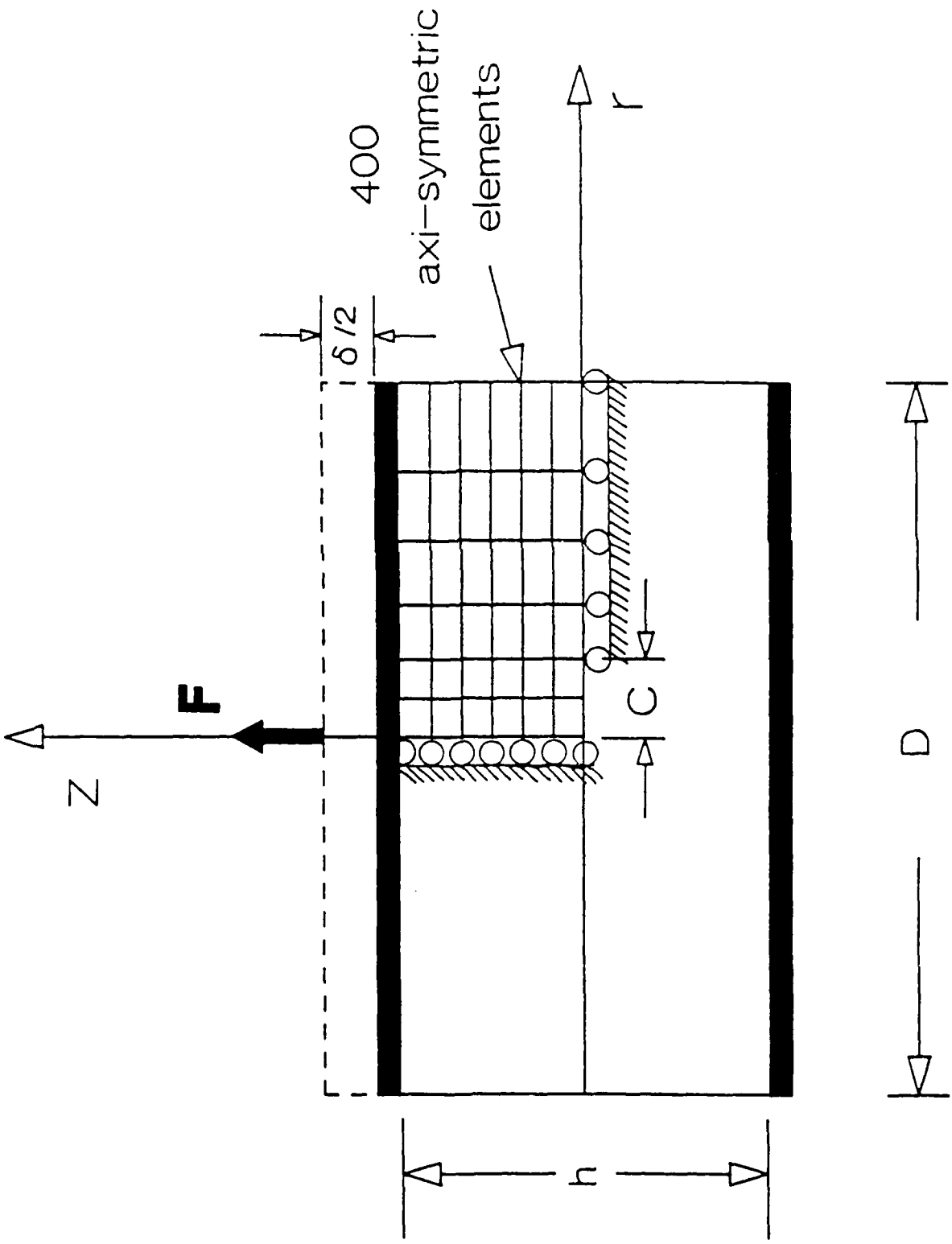

Figure 4

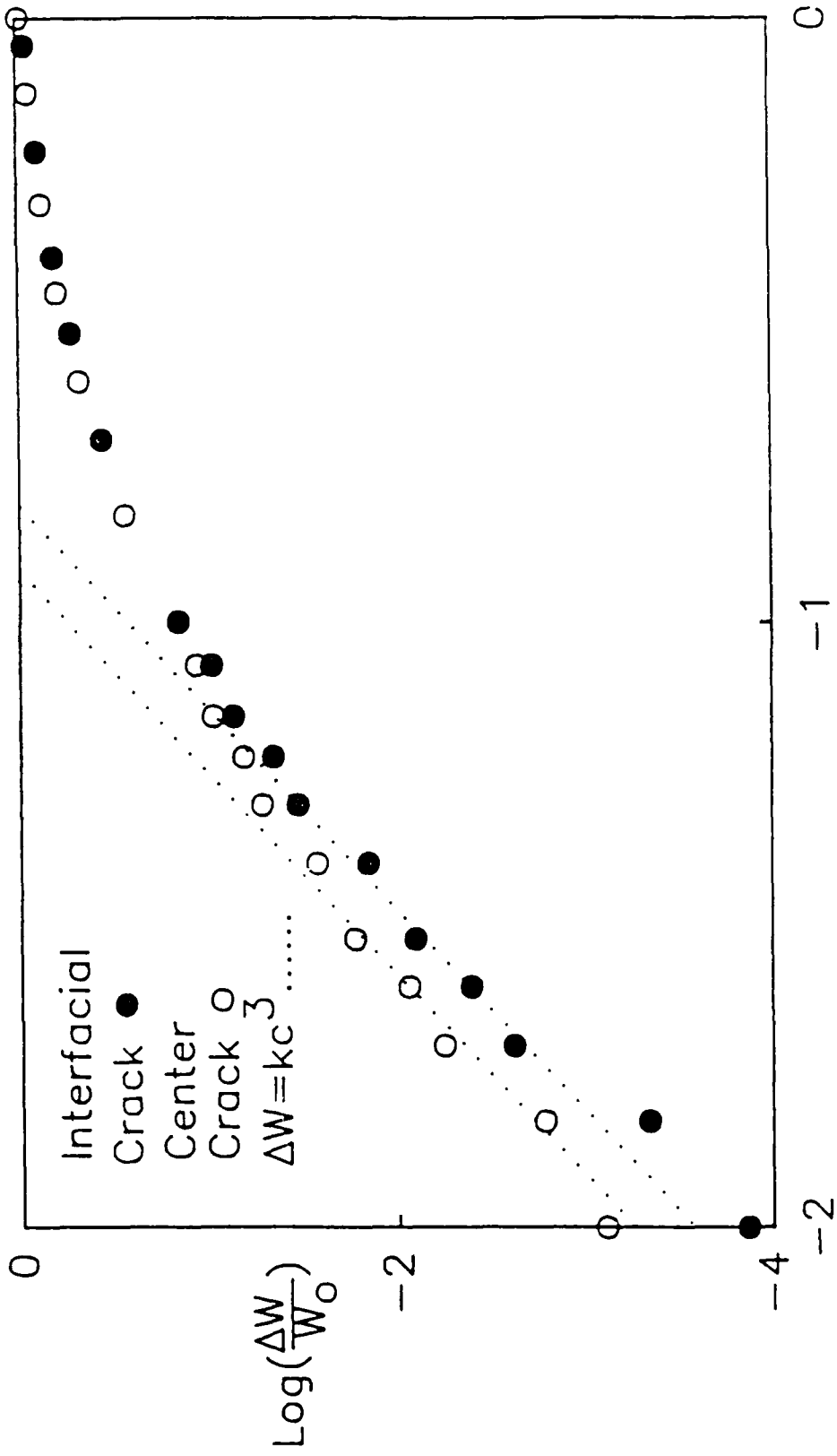
Interfacial Crack
Center Crack
$\Delta W = kc^3$
$\text{Log}(\frac{\Delta W}{W_o})$
0
−2
−4
0
−1
−2
Log (c/a)

Figure 5

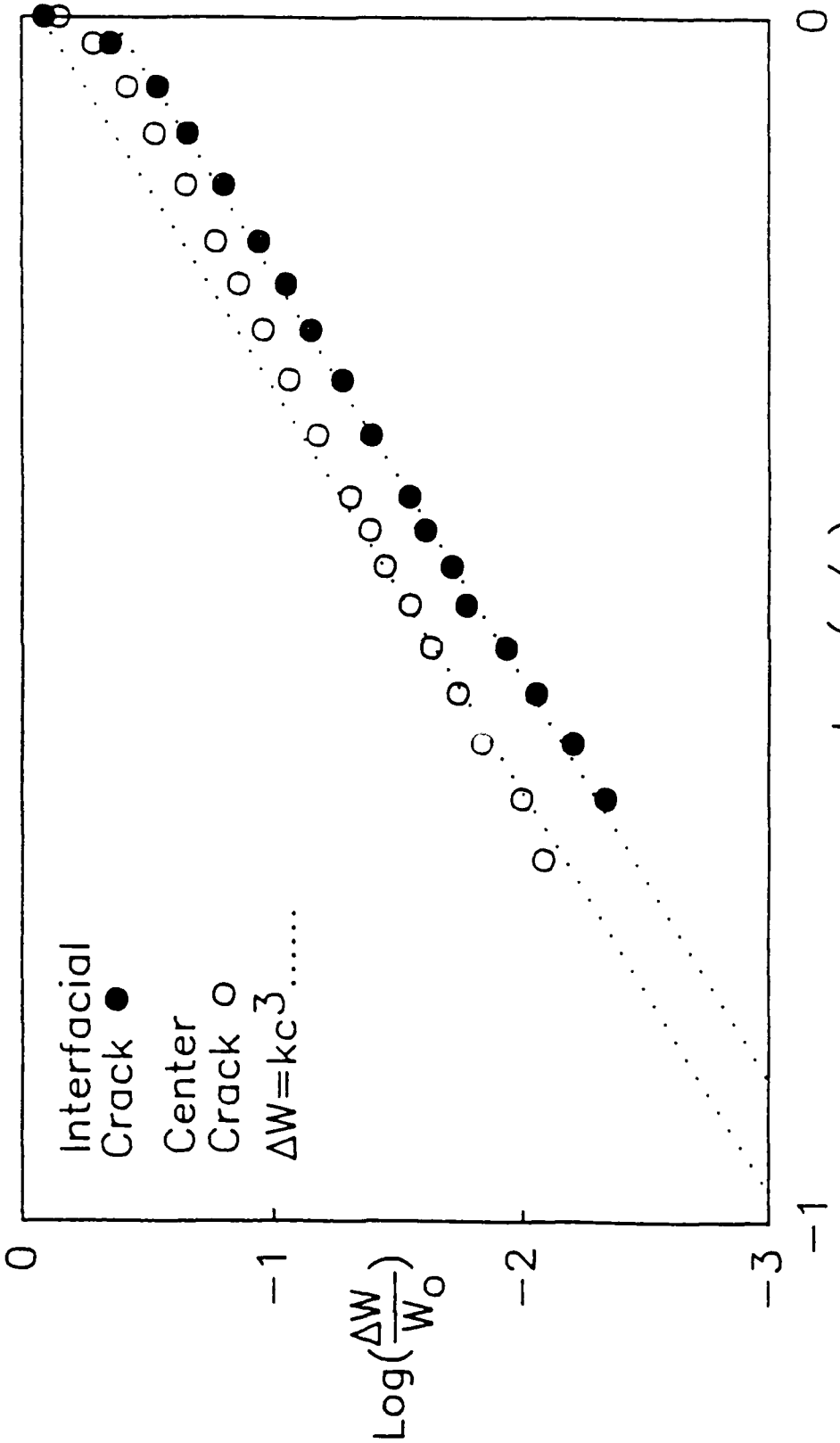
Interfacial Crack ●
Center Crack o
ΔW=kc^3.....
Log(ΔW/W_o)
0
−1
−2
−3
0
−1
Log (c/a)

Figure 6

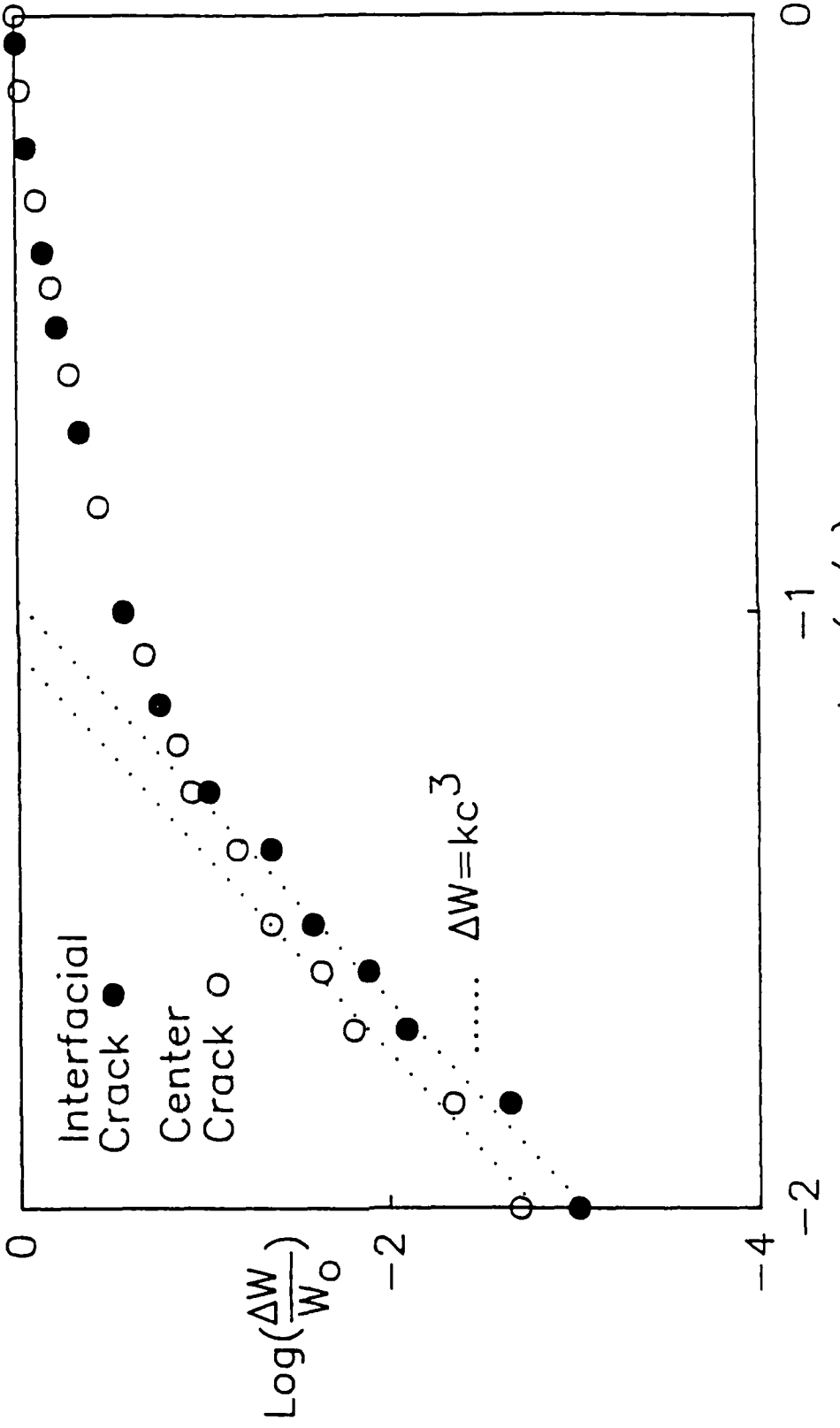
Interfacial Crack
Center Crack
$\Delta W = kc^3$
$\text{Log}(\frac{\Delta W}{W_o})$
Log(c/a)
0
−2
−4
0
−1
−2

Figure 7

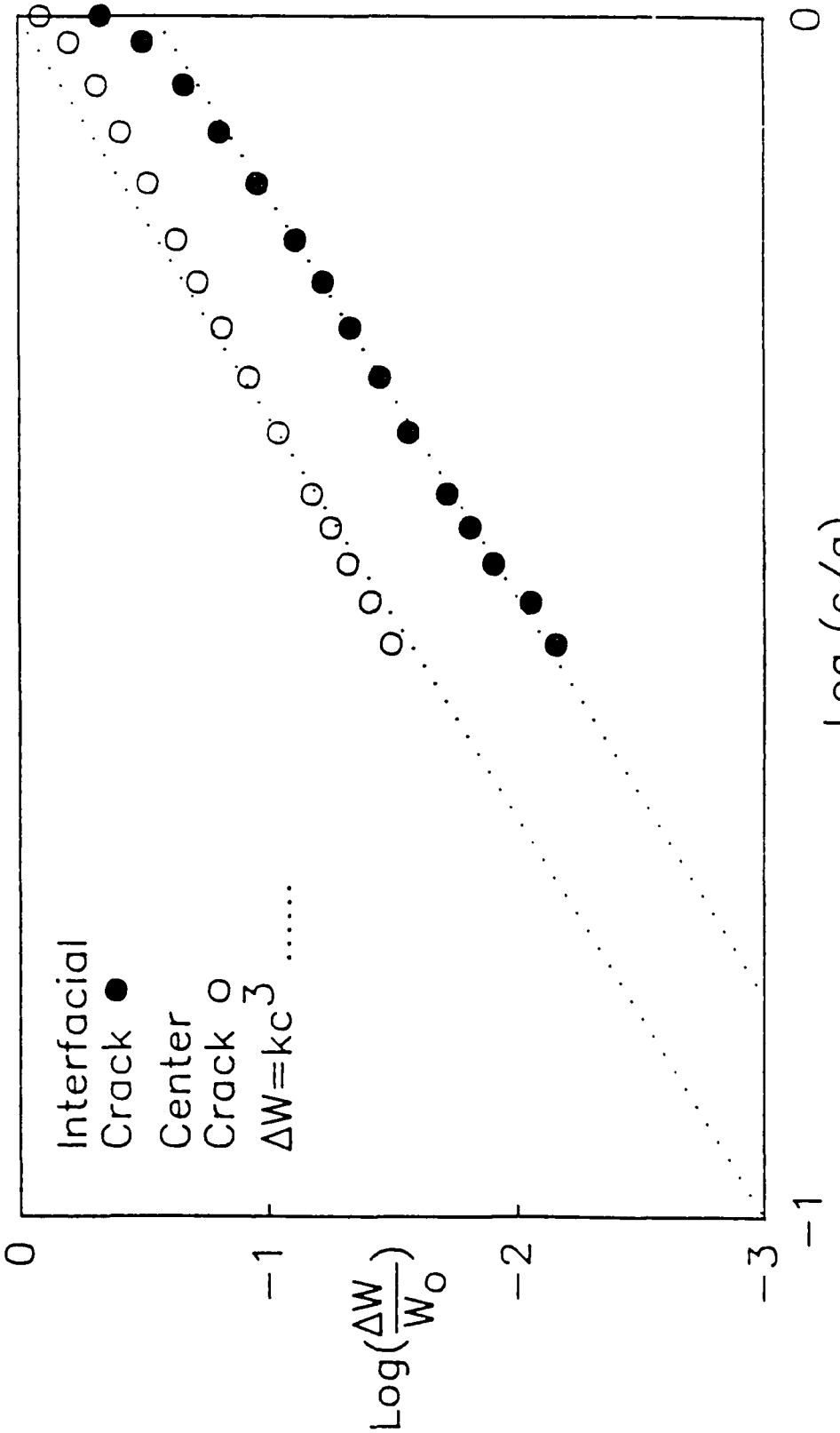
Interfacial
Crack ●
Center
Crack o
ΔW=kc^3
0
−1
−2
−3
Log(ΔW/W_o)
0
−1
Log (c/a)

Figure 8

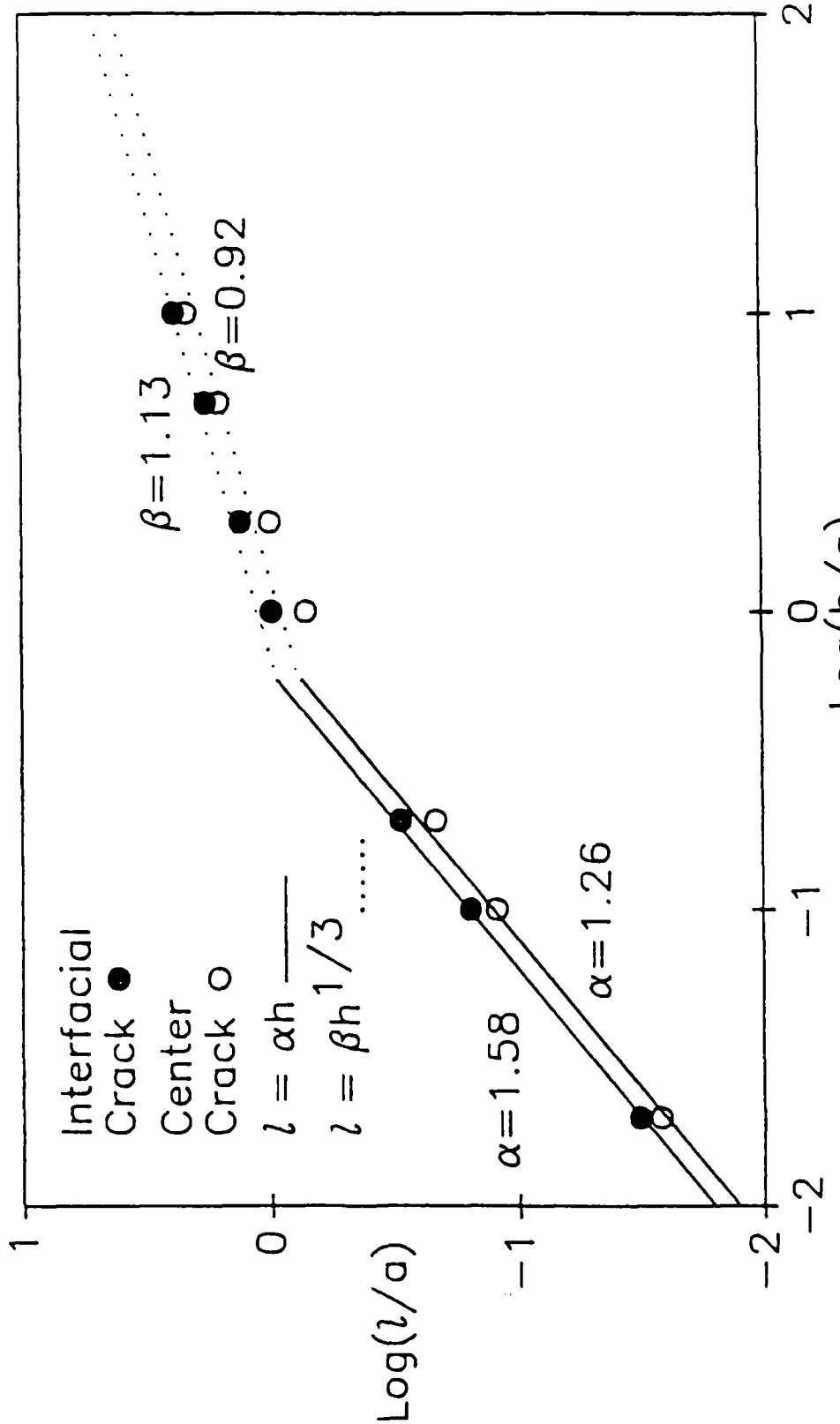
Interfacial Crack ●
Center Crack o
$l = \alpha h$
$l = \beta h^{1/3}$
β=1.13
β=0.92
α=1.58
α=1.26
Log(l/a)
Log(h/a)
1
0
−1
−2
2

Figure 9

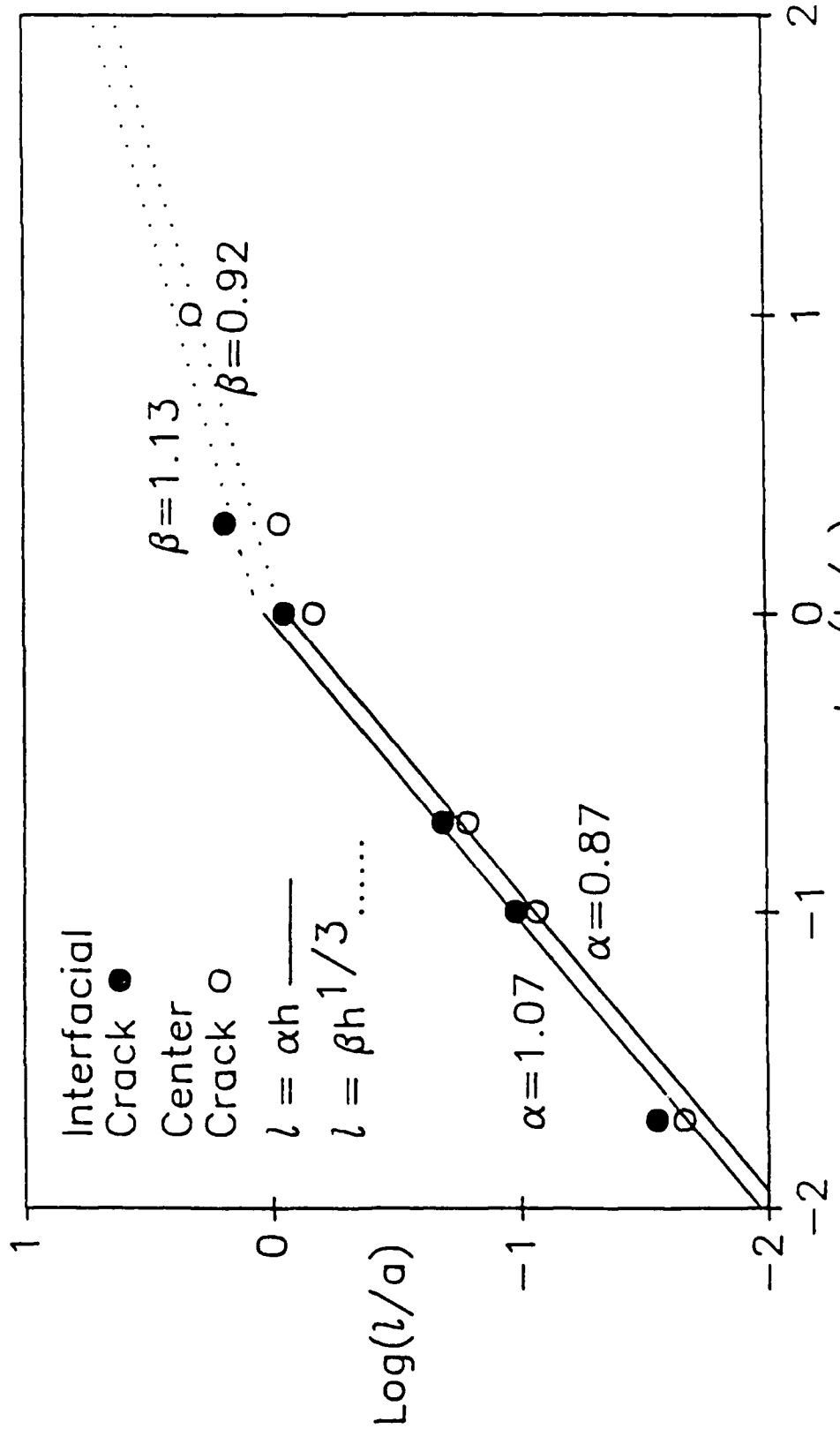
Interfacial Crack ●
Center Crack o
$l = \alpha h$ ——
$l = \beta h^{1/3}$ .....
α=1.07
α=0.87
β=1.13
β=0.92
Log(l/a)
Log(h/a)
1
0
−1
−2
2

Figure 10

(DYN)

DISTRIBUTION LIST

Dr. R.S. Miller
Office of Naval Research
Code 432P
Arlington, VA 22217
(10 copies)

Dr. J. Pastine
Naval Sea Systems Command
Code 06R
Washington, DC 20362

Dr. Kenneth D. Hartman
Hercules Aerospace Division
Hercules Incorporated
Alleghany Ballistic Lab
P.O. Box 210
Cumberland, MD 20502

Mr. Otto K. Heiney
AFATL-DLJG
Elgin AFB, FL 32542

Dr. Merrill K. King
Atlantic Research Corp.
5390 Cherokee Avenue
Alexandria, VA 22312

Dr. R.L. Lou
Aerojet Strategic Propulsion Co.
Bldg. 05025 - Dept 5400 - MS 167
P.O. Box 15699C
Sacramenta, CA 95813

Dr. R. Olsen
Aerojet Strategic Propulsion Co.
Bldg. 05025 - Dept 5400 - MS 167
P.O. Box 15699C
Sacramento, CA 95813

Dr. Randy Peters
Aerojet Strategic Propulsion Co.
Bldg. 05025 - Dept 5400 - MS 167
P.O. Box 15699C
Sacramento, CA 95813

Dr. D. Mann
U.S. Army Research Office
Engineering Division
Box 12211
Research Triangle Park, NC 27709-2211

Dr. L.V. Schmidt
Office of Naval Technology
Code 07CT
Arlington, VA 22217

JHU Applied Physics Laboratory
ATTN: CPIA (Mr. T.W. Christian)
Johns Hopkins Rd.
Laurel, MD 20707

Dr. R. McGuire
Lawrence Livermore Laboratory
University of California
Code L-324
Livermore, CA 94550

P.A. Miller
736 Leavenworth Street, #6
San Francisco, CA 94109

Dr. W. Moniz
Naval Research Lab.
Code 6120
Washington, DC 20375

Dr. K.F. Mueller
Naval Surface Weapons Center
Code R11
White Oak
Silver Spring, MD 20910

Prof. M. Nicol
Dept. of Chemistry & Biochemistry
University of California
Los Angeles, CA 90024

Mr. L. Roslund
Naval Surface Weapons Center
Code R10C
White Oak, Silver Spring, MD 20910

Dr. David C. Sayles
Ballistic Missile Defense
Advanced Technology Center
P.O. Box 1500
Huntsville, AL 35807

(DYN)

DISTRIBUTION LIST

Mr. R. Geisler
ATTN: DY/MS-24
AFRPL
Edwards AFB, CA 93523

Naval Air Systems Command
ATTN: Mr. Bertram P. Sobers
NAVAIR-320G
Jefferson Plaza 1, RM 472
Washington, DC 20361

R.B. Steele
Aerojet Strategic Propulsion Co.
P.O. Box 15699C
Sacramento, CA 95813

Mr. M. Stosz
Naval Surface Weapons Center
Code R10B
White Oak
Silver Spring, MD 20910

Mr. E.S. Sutton
Thiokol Corporation
Elkton Division
P.O. Box 241
Elkton, MD 21921

Dr. Grant Thompson
Morton Thiokol, Inc.
Wasatch Division
MS 240 P.O. Box 524
Brigham City, UT 84302

Dr. R.S. Valentini
United Technologies Chemical Systems
P.O. Box 50015
San Jose, CA 95150-0015

Dr. R.F. Walker
Chief, Energetic Materials Division
DRSMC-LCE (D), B-3022
USA ARDC
Dover, NJ 07801

Dr. Janet Wall
Code 012
Director, Research Administration
Naval Postgraduate School
Monterey, CA 93943

Director
US Army Ballistic Research Lab.
ATTN: DRXBR-IBD
Aberdeen Proving Ground, MD 21005

Commander
US Army Missile Command
ATTN: DRSMI-RKL
Walter W. Wharton
Redstone Arsenal, AL 35898

Dr. Ingo W. May
Army Ballistic Research Lab.
ARRADCOM
Code DRXBR - IBD
Aberdeen Proving Ground, MD 21005

Dr. E. Zimet
Office of Naval Technology
Code 071
Arlington, VA 22217

Dr. Ronald L. Derr
Naval Weapons Center
Code 389
China Lake, CA 93555

T. Boggs
Naval Weapons Center
Code 389
China Lake, CA 93555

Lee C. Estabrook, P.E.
Morton Thiokol, Inc.
P.O. Box 30058
Shreveport, Louisiana 71130

Dr. J.R. West
Morton Thiokol, Inc.
P.O. Box 30058
Shreveport, Louisiana 71130

Dr. D.D. Dillehay
Morton Thiokol, Inc.
Longhorn Division
Marshall, TX 75670

G.T. Bowman
Atlantic Research Corp.
7511 Wellington Road
Gainesville, VA 22065

(DYN)

DISTRIBUTION LIST

R.E. Shenton
Atlantic Research Corp.
7511 Wellington Road
Gainesville, VA 22065

Brian Wheatley
Atlantic Research Corp.
7511 Wellington Road
Gainesville, VA 22065

Mike Barnes
Atlantic Research Corp.
7511 Wellington Road
Gainesville, VA 22065

Mr. G. Edwards
Naval Sea Systems Command
Code 62R32
Washington, DC 20362

Dr. Lionel Dickinson
Naval Explosive Ordinance
Disposal Tech. Center
Code D
Indian Head, MD 20340

C. Dickinson
Naval Surface Weapons Center
White Oak, Code R-13
Silver Spring, MD 20910

Prof. J.T. Dickinson
Washington State University
Dept. of Physics 4
Pullman, WA 99164-2814

Prof. John Deutch
MIT
Department of Chemistry
Cambridge, MA 02139

M.H. Miles
Dept. of Physics
Washington State University
Pullman, WA 99164-2814

Dr. E.H. deButts
Hercules Aerospace Co.
P.O. Box 27408
Salt Lake City, UT 84127

Dr. T.F. Davidson
Vice President, Technical
Morton Thiokol, Inc.
Aerospace Group
3340 Airport Rd.
Ogden, UT 84405

David A. Flanigan
Director, Advanced Technology
Morton Thiokol, Inc.
Aerospace Group
3340 Airport Rd.
Ogden, UT 84405

Mr. J. Consaga
Naval Surface Weapons Center
Code R-16
Indian Head, MD 20640

Dr. L.H. Caveny
Air Force Office of Scientific
Research
Directorate of Aerospace Sciences
Bolling Air Force Base
Washington, DC 20332

Naval Sea Systems Command
ATTN: Mr. Charles M. Christensen
NAVSEA-62R2
Crystal Plaza, Bldg. 6, Rm 806
Washington, DC 20362

W.G. Roger
Code 5253
Naval Ordance Station
Indian Head, MD 20640

Mr. R. Beauregard
Naval Sea Systems Command
SEA 64E
Washington, DC 20362

Dr. Donald L. Ball
Air Force Office of Scientific
Research
Directorate of Chemical &
Atmospheric Sciences
Bolling Air Force Base
Washington, DC 20332

(DYN)

DISTRIBUTION LIST

Dr. Anthony J. Matuszko
Air Force Office of Scientific Research
Directorate of Chemical & Atmospheric Sciences
Bolling Air Force Base
Washington, DC 20332

Dr. Michael Chaykovsky
Naval Surface Weapons Center
Code R11
White Oak
Silver Spring, MD 20910

J.J. Rocchio
USA Ballistic Research Lab.
Aberdeen Proving Ground, MD 21005-5066

Dr. H.G. Adolph
Naval Surface Weapons Center
Code R11
White Oak
Silver Spring, MD 20910

U.S. Army Research Office
Chemical & Biological Sciences Division
P.O. Box 12211
Research Triangle Park, NC 27709

Dr. John S. Wilkes, Jr.
FJSRL/NC
USAF Academy, CO 80840

Dr. H. Rosenwasser
AIR-320R
Naval Air Systems Command
Washington, DC 20361

B. Swanson
INC-4 MS C-346
Los Alamos National Laboratory
Los Alamos, New Mexico 87545

Dr. James T. Bryant
Naval Weapons Center
Code 3205B
China Lake, CA 93555

Dr. L. Rothstein
Assistant Director
Naval Explosives Dev. Engineering Dept.
Naval Weapons Station
Yorktown, VA 23691

Dr. M.J. Kamlet
Naval Surface Weapons Center
Code R11
White Oak, Silver Spring, MD 20910

Dr. Henry Webster, III
Manager, Chemical Sciences Branch
ATTN: Code 5063
Crane, IN 47522

Dr. A.L. Slafkosky
Scientific Advisor
Commandant of the Marine Corps
Code RD-1
Washington, DC 20380

Dr. Joyce J. Kaufman
The Johns Hopkins University
Department of Chemistry
Baltimore, MD 21218

Dr. A. Nielsen
Naval Weapons Center
Code 385
China Lake, CA 93555

(DYN)

DISTRIBUTION LIST

K.D. Pae
High Pressure Materials Research Lab.
Rutgers University
P.O. Box 909
Piscataway, NJ 08854

Dr. John K. Dienes
T-3, B216
Los Alamos National Lab.
P.O. Box 1663
Los Alamos, NM 87544

A.N. Gent
Institute Polymer Science
University of Akron
Akron, OH 44325

Dr. D.A. Shockey
SRI International
333 Ravenswood Ave.
Menlo Park, CA 94025

Dr. R.B. Kruse
Morton Thiokol, Inc.
Huntsville Division
Huntsville, AL 35807-7501

G. Butcher
Hercules, Inc.
P.O. Box 98
Magna, UT 84044

W. Waesche
Atlantic Research Corp.
7511 Wellington Road
Gainesville, VA 22065

Dr. R. Bernecker
Naval Surface Weapons Center
Code R13
White Oak
Silver Spring, MD 20910

Prof. Edward Price
Georgia Institute of Tech.
School of Aerospace Engineering
Atlanta, GA 30332

J.A. Birkett
Naval Ordnance Station
Code 5253K
Indian Head, MD 20640

Prof. R.W. Armstrong
University of Maryland
Dept. of Mechanical Engineering
College Park, MD 20742

Herb Richter
Code 385
Naval Weapons Center
China Lake, CA 93555

J.T. Rosenberg
SRI International
333 Ravenswood Ave.
Menlo Park, CA 94025

G.A. Zimmerman
Aeroject Tactical Systems
P.O. Box 13400
Sacramento, CA 95813

Prof. Kenneth Kuo
Pennsylvania State University
Dept. of Mechanical Engineering
University Park, PA 16802

T.L. Boggs
Naval Weapons Center
Code 3891
China Lake, CA 93555

(DYN)

DISTRIBUTION LIST

Dr. C.S. Coffey
Naval Surface Weapons Center
Code R13
White Oak
Silver Spring, MD 20910

D. Curran
SRI International
333 Ravenswood Avenue
Menlo Park, CA 94025

E.L. Throckmorton
Code SP-2731
Strategic Systems Program Office
Crystal Mall #3, RM 1048
Washington, DC 23076

R.G. Rosemeier
Brimrose Corporation
7720 Belair Road
Baltimore, MD 20742

C. Gotzmer
Naval Surface Weapons Center
Code R-11
White Oak
Silver Spring, MD 20910

G.A. Lo
3251 Hanover Street
B204 Lockheed Palo Alto Research Lab
Palto Alto, CA 94304

R.A. Schapery
Civil Engineering Department
Texas A&M University
College Station, TX 77843

Dr. Y. Gupta
Washington State University
Department of Physics
Pullman, WA 99163

J.M. Culver
Strategic Systems Projects Office
SSPO/SP-2731
Crystal Mall #3, RM 1048
Washington, DC 20376

Prof. G.D. Duvall
Washington State University
Department of Physics
Pullman, WA 99163

Dr. E. Martin
Naval Weapons Center
Code 3858
China Lake, CA 93555

Dr. M. Farber
135 W. Maple Avenue
Monnovia, CA 91016

W.L. Elban
Naval Surface Weapons Center
White Oak, Bldg. 343
Silver Spring, MD 20910

Defense Technical Information Center
Bldg. 5, Cameron Station
Alexandria, VA 22314
(12 copies)

Dr. Robert Polvani
National Bureau of Standards
Metallurgy Division
Washington, D.C. 20234

Director
Naval Research Laboratory
Attn: Code 2627
Washington, DC 20375
(6 copies)

Administrative Contracting
Officer (see contract for
address)
(1 copy)